Supplementary Material

Recognition of a key anchor residue by a conserved hydrophobic pocket ensures subunit interface integrity in DNA clamps

Senthil K. Perumal[a,c,d], Xiaojun Xu[b,c,e], , Chunli Yan[b], Ivaylo Ivanov[b,1], Stephen J. Benkovic[a,1]

[a]Department of Chemistry, 414 Wartik Laboratory, The Pennsylvania State University, University Park, PA 16802 USA. [b]Department of Chemistry and Center for Diagnostics and Therapeutics, Georgia State University, Atlanta, GA 30302, USA. [d]Ideaya Biosciences, South San Francisco, CA 94080. [e]Moores Cancer Center, University of California, San Diego, CA 92093.

[1]To whom all correspondence should be addressed, Email: sjb1@psu.edu, Phone: (814) 865-2882, Fax: (814) 865-2973. Correspondence may also be addressed to Ivaylo Ivanov. Email: iivanov@gsu.edu; Tel: +1 404 413 5529; Fax: +1 404 413 5505. [c] Equal contribution.

[d,e] Present address

Table S1. Primers used to generate PCNA mutations

Mutation	Mutagenic Primers
C27M W28F	CTCATCAACGAGGCCATGTGGGATATTAGC
C27S W28F	CTCATCAACGAGGCCTCGTGGGATATTAGC
C62M	TTCGACACCTACCGCATGGACCGCAACCTG
C62S	TTCGACACCTACCGCTCGGACCGCAACCTG
C81S	CCAAAATACTAAAATCGGCCGGCAATGAAG
C135S	AGAACAGGAGTACAGCTCGGTAGTAAAGATG
C148S	TTTGCACGTATATCGCGAGATCTCAGCCAT
C162S	GATGCTGTTGTAATTTCCTCGGCAAAAGACGGAGTG
N107W	CTAGTATTTGAAGCACCATGGCAGGAGAAAGTTTCAG
N107C	CTAGTATTTGAAGCACCATGCCAGGAGAAAGTTTCAG
N185C	AAATTGTCACAGTGCAGTAATGTCGATAAAGAGGAGG
N185W	AAATTGTCACAGTGGAGTAATGTCGATAAAGAGGAGG

Table S2. Relative ATPase activity of RFC PCNA complexes

Clamp added to RFC•DNA complex	Relative rate of ATP hydrolysis (% activity)
PCNA wild type	100
PCNA-WC1 or PCNA-WC2	83 ± 12
PCNA-WC-AEDANS	80 ± 15

Table S3. NCBI accession numbers of the sliding clamps used in the multiple sequence alignment

Organism	**Accession number**
Human PCNA	NP_002583.1
Rhesus Monkey	EHH19900.1
Dog	XP_534355.3
Guinea Pig	XP_003476647.1
Mouse	NP_035175.1
Chicken	NP_989501.1
Zebra Fish	AAF18324.1
Xenopus	P18248.1
Drosophila	NP_476905.1
Yeast	NP_009645.1
Salmonella typhi	WP_000673474.1
Klebsiella pneumoniae	WP_004145090.1
E. coli	WP_000673464.1
Enterobacter cloacae	WP_015570134.1
Proteus mirabilis	WP_004246506.1
Acinetobacter baumannii	WP_001237348.1
Mycobacterium tuberculosis	WP_003400271.1
Corynebacterium diphtheriae	WP_003853309.1
Listeria monocytogenes	WP_003725616.1
S. aureus	WP_000969811.1
T4-gp45	NP_049666.1
RB32-gp45	WP_015983598.1
Cc31-gp45	YP_004009906.1
RB69-gp45	WP_015971447.1
JS98-gp45	YP_003934678.1

Table S4. Kinetics of PCNA clamp protein subunit exchange

Protein components	Rate of subunit exchange* (k_{ex}, $x10^{-4}$ s^{-1})
200 nM PCNA-WC1-AEDANS	12.5 ± 3.2
200 nM PCNA-WC1-AEDANS, 200 nM RFC, 10 mM ATP	8.8 ± 1.5
200 nM PCNA-WC1-AEDANS, 200 nM RFC, 200 nM Bio23/62/36, 1000 nM avidin, 10 mM ATP	9.5 ± 2.3
200 nM PCNA-WC1-AEDANS, 200 nM RFC, 200 nM Pol δ, 200 nM Bio23/62/36, 1000 nM avidin, 10 mM ATP	4.2 ± 1.2

*Kinetics of PCNA subunit exchange were monitored by mixing the protein components against 2 μM PCNA-W28F trap protein in the reaction buffer (pH 7.8) at 25 °C. Rate constant were obtained by fitting experimental data to a single exponential equation.

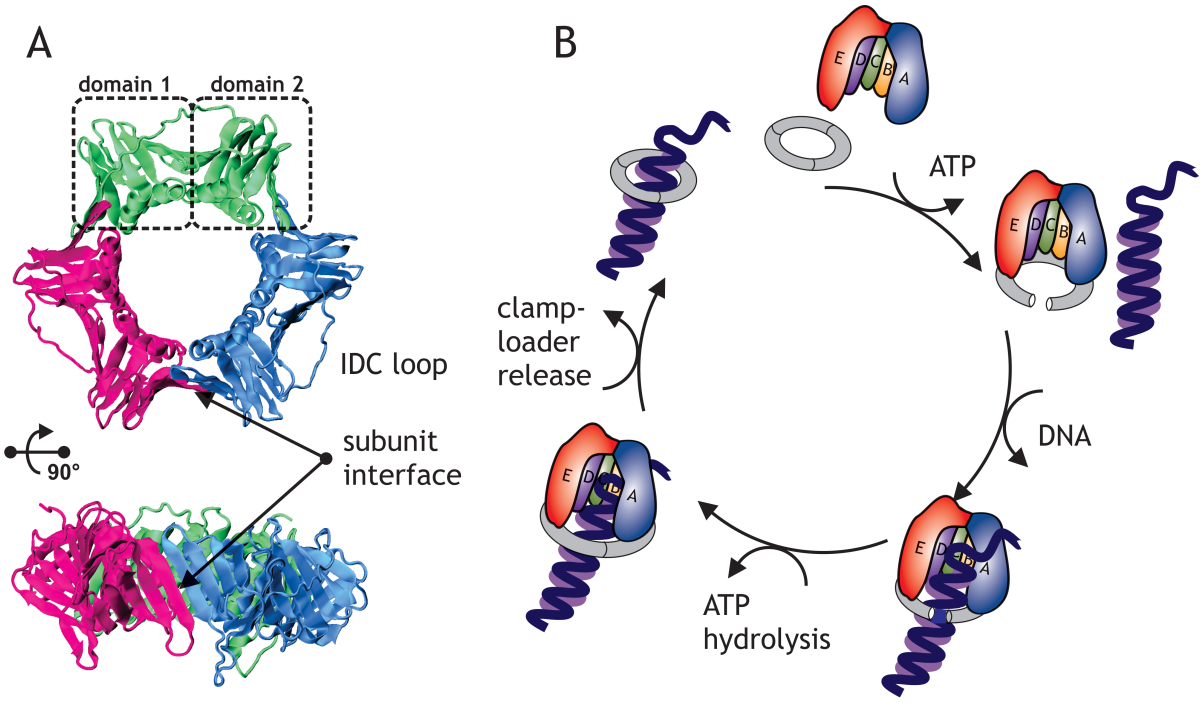

Figure S1. Overview of (a) the human PCNA (1VYM) and the subunit interface; (b) Clamp-loading process facilitated by the clamp loader. The five-subunit clamp loader associates and opens PCNA subunit-subunit interface for the subsequent double-strand DNA loading in the presence of ATP; The ATP hydrolyzation then drives the ring-closing and the dissociation of the clamp loader.

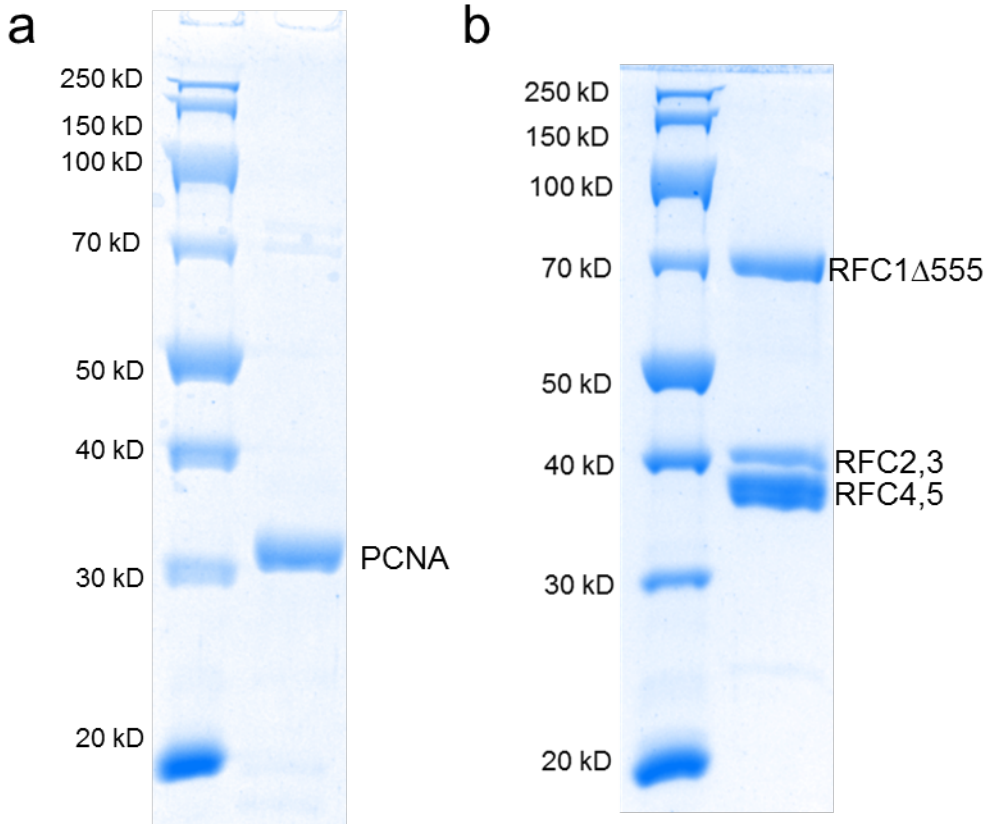

Figure S2. Characterization of (a) human PCNA-WC1 mutant and (b) human RFC proteins. Proteins were expressed and purified as described in Methods. Purified proteins were resolved on a 10% SDS PAGE gel.

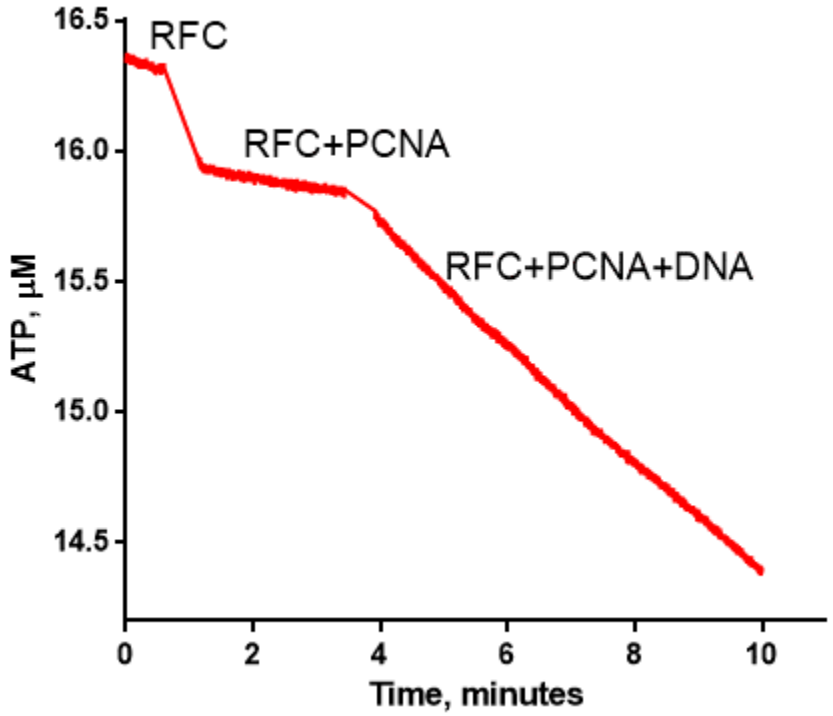

Figure S3. Assaying PCNA-dependent ATPase activity of RFC in the presence of DNA. Addition of PCNA (200 nM) stimulated ATP (2 mM) turnover by RFC (200 nM) in the presence of Bio23/62/36 forked DNA (200 nM) and avidin (1 μM) in the reaction buffer (pH 7.8) at 25 °C. ATP hydrolysis was measured using NADH-oxidation coupled enzymatic assay monitored at 340 nm.

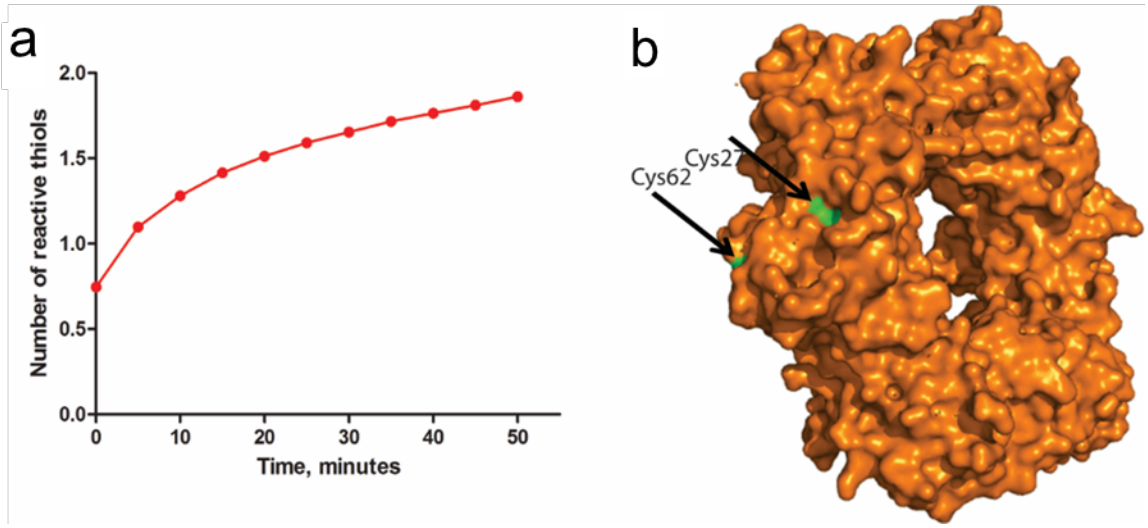

Figure S4. (a) Evaluation of reactive cysteines of wild type PCNA. Monomeric wt PCNA (4 μM) was treated with 5,5'-dithio-bis-(2-nitrobenzoic acid) (DTNB, 2 mM) in 20 mM phosphate buffer (pH 7.6), 50 mM NaCl at 25 °C and the reaction was monitored at 412 nm. The number of reactive thiols were calculated using the extinction coefficient of 13600 M^{-1} cm^{-1} at 412 nm. (b) Assignment of the two reactive thiols to Cys27 and Cys62 (colored in green) that are solvent exposed in the crystal structure.

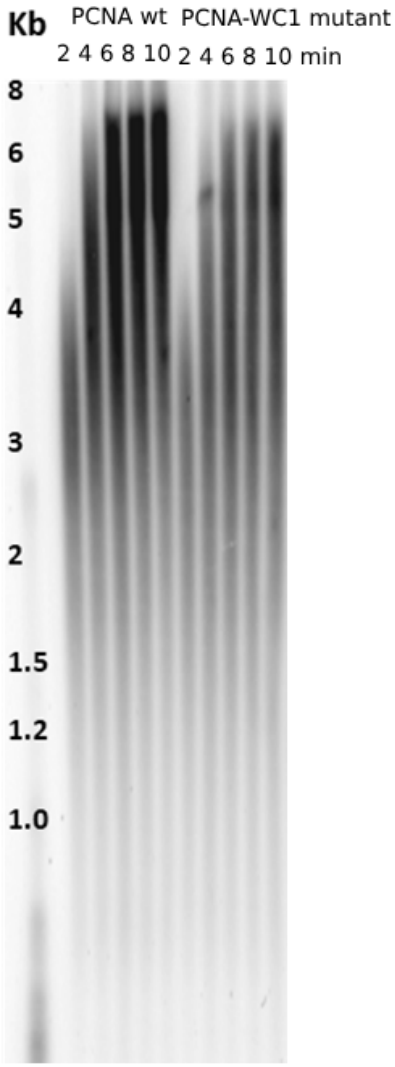

Figure S5. Primer Extension assay was carried out in the reaction buffer at 37°C. The 38 nucleotide long primer (5'-GGG TTT TCC CAG TCA CGA GGT TGT AAA ACG ACG GCC AG-3', which is complementary to the 6328-6291 region of ssM13mp18 DNA) was annealed to ssM13 DNA at a ratio of 2:1. The reaction mixture contained 10 nM singly-primed ssM13 DNA, 100 nM Pol δ, 100 nM RFC, 200 nM PCNA-wt or PCNA-WC1 mutant, 2 μM RPA, 50 μM dNTPs (10 μCi α-^{32}P-dCTP was added), and 1 mM ATP. The reactions were quenched with 2x loading buffer (60 mM NaOH, 2 mM EDTA) at regular intervals and the products were resolved on a 0.8 % alkaline agarose gel, transferred to DE81 paper, exposed to a PhosphoImager screen, and quantified by ImageQuant.

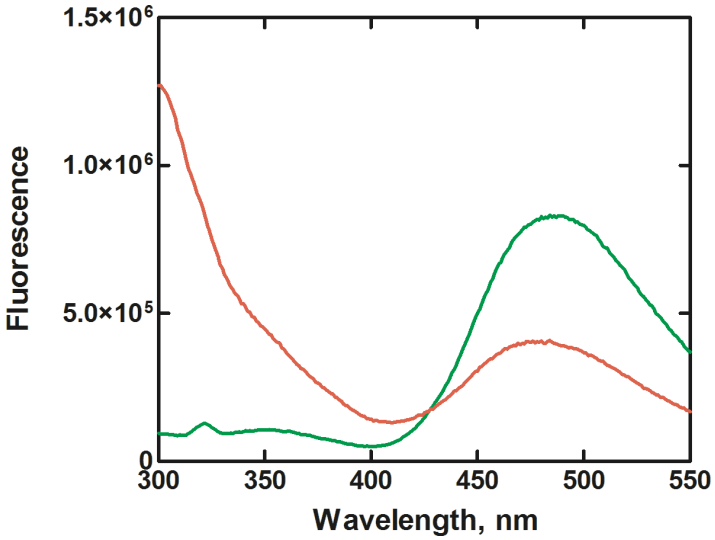

Figure S6. Solution exchange of human PCNA clamp subunits measured by steady state fluorescence resonance energy transfer. Fluorescence emission spectrum of 200 nM PCNA-WC1-AEDANS alone (*green*) and in the presence of 2 μM PCNA trap protein lacking Trp at the subunit interface (*red*) incubated for 15 min in the reaction buffer (pH 7.8) at 25 °C. Significant drop in the FRET signal confirmed the exchange of subunits in solution.

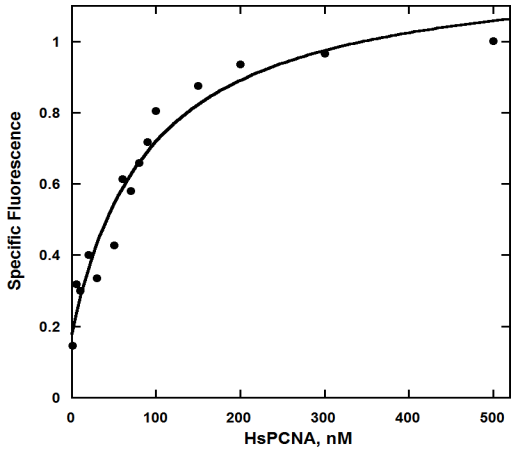

Figure S7. Oligomerization of the human PCNA protein in the reaction buffer (pH 7.8) at 25 °C. Fluorescence emission at 480 nm was monitored using 290 nm excitation at various concentrations of PCNA. The concentration of the PCNA-WC1-AEDANS protein was varied from 2 to 500 nM in reaction buffer with BSA (100 nM) as a carrier protein. Each concentration was equilibrated at

25 °C for approximately 1 h prior to the fluorescence observation. The solid line represents the fit to scheme 1 using Dynafit3.

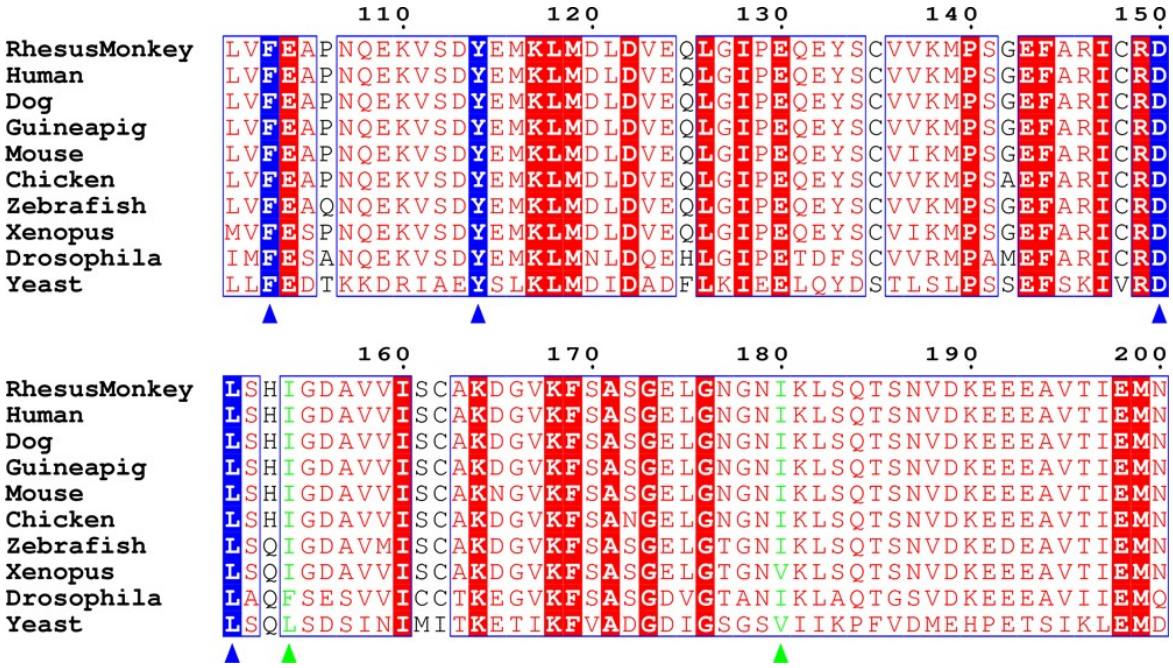

Figure S8. Primary sequence alignment of eukaryotic DNA sliding clamp proteins. Protein sequences for eukaryotic clamp proteins were retrieved from the NCBI server by their accession numbers listed in Table S3. The clamp proteins were then aligned using CLUSTALW multiple sequence alignment tool in Biology WorkBench available from San Diego Supercomputer Center. The aligned sequences, exported as FASTA multiple sequence files, were then used to generate color-coded plots displaying various single, fully conserved residue and conservation of strong and weak groups in the multiple sequence alignment using ExPASy Bioinformatics Resources Portal tool from the Swiss Institute of Bioinformatics.

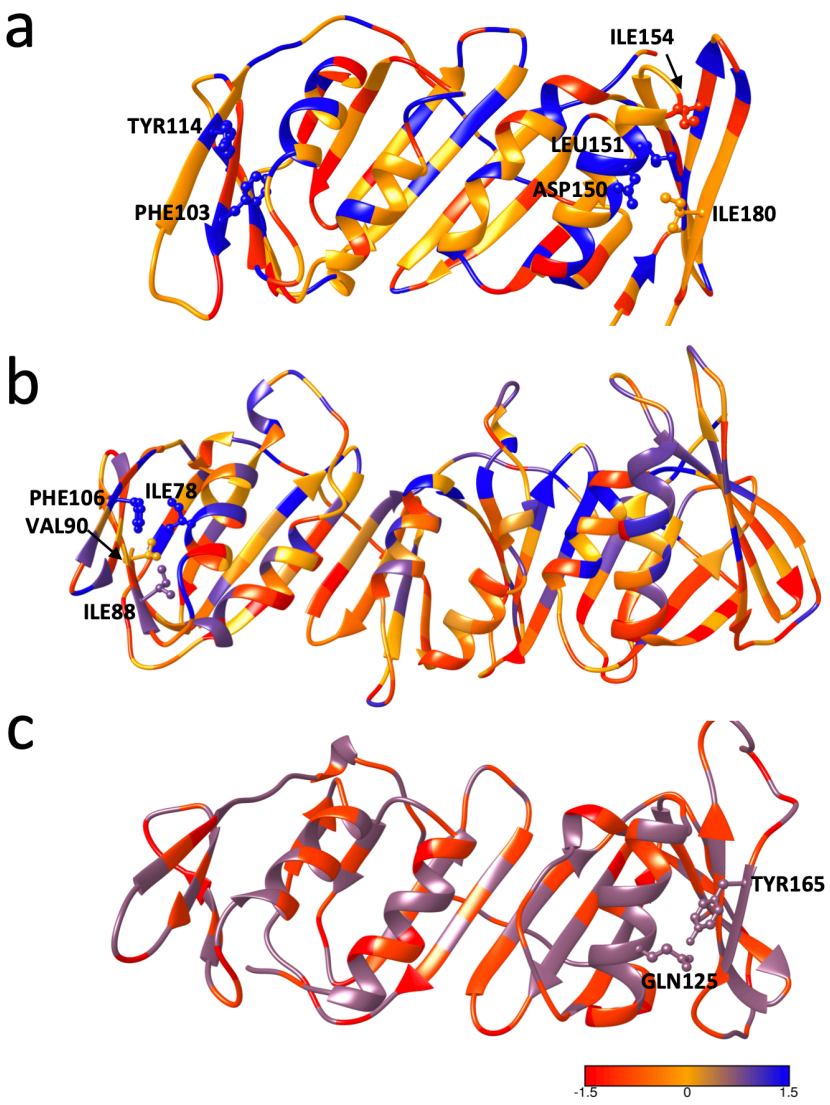

Figure S9. Sequence conservation mapped onto the clamp monomer proteins using the corresponding alignment profile generated with the sequences in Table S3. (a) Eukaryotic clamp conservation mapped to human PCNA (1VYM); (b) Prokaryotic clamp conservation mapped to *E. coli* β-clamp (2POL); (c) bacteriophage gp45 clamp conservation mapped to *T4* phage gp45 clamp (3U6O). Residue conservation is color-coded from red (*low*) to blue (*high*). Conserved residues involved in forming the hydrophobic pocket complementary to the anchoring residue are labeled.

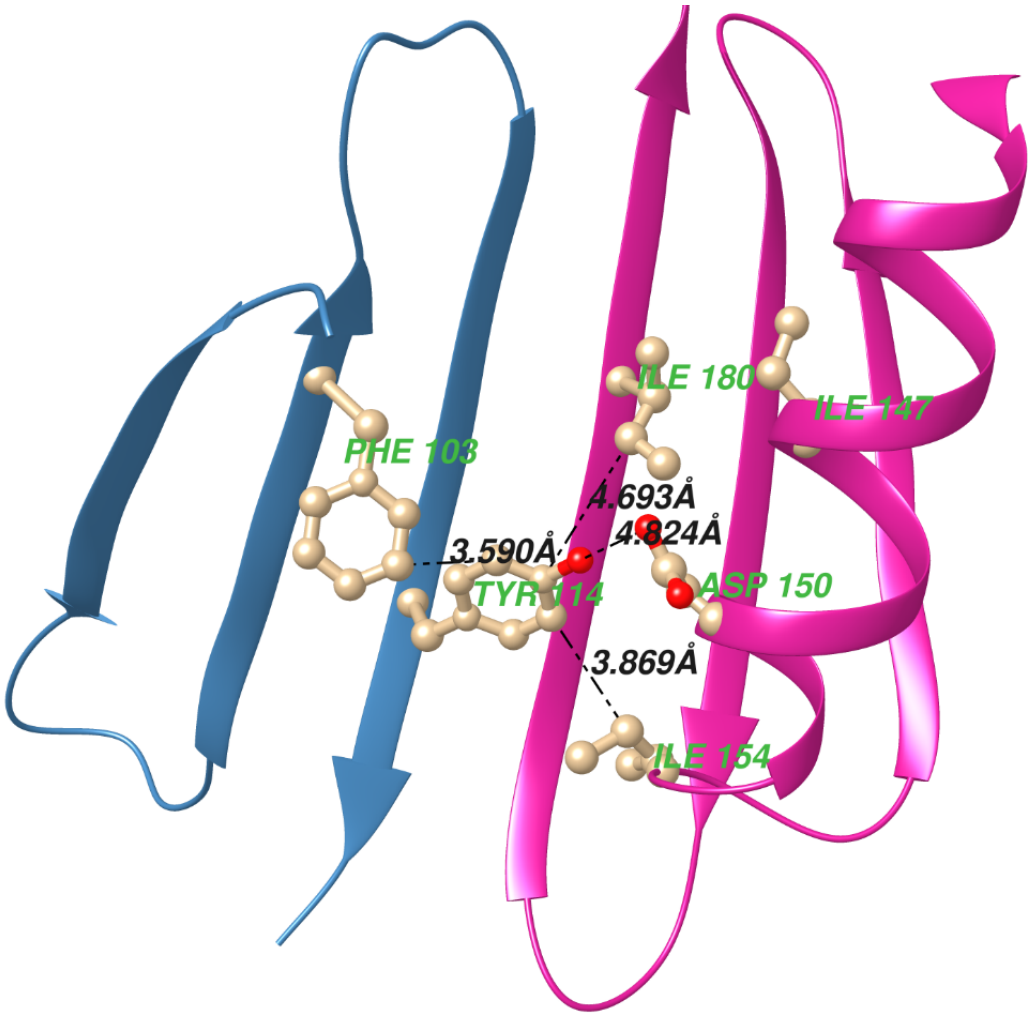

Figure S10. Subunit interface organization of human PCNA clamp. Hydrophobic aggregation of side chains of residues at the subunit interface.

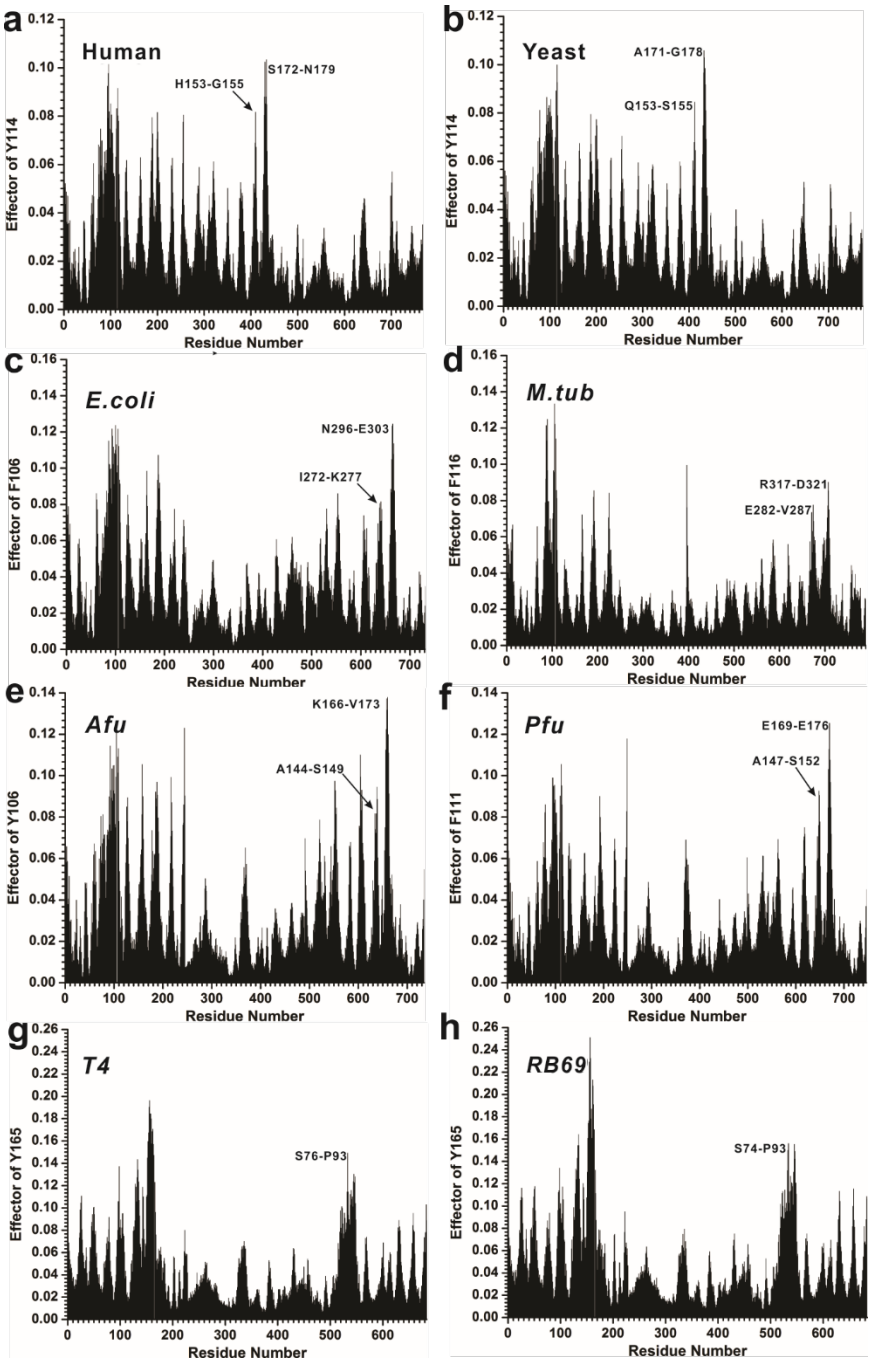

Figure S11. Effectiveness/influence profile obtained upon unit perturbation on the tyrosine or phenylalanine anchor residue using PRS analysis a) Human PCNA; b) Yeast PCNA; c) *E. coli* β-clamp; d) *M.tub* clamp; e) *Afu* PCNA; f) *Pfu* PCNA; g) *T4* gp45; h) *RB69* gp45. Peaks of the opposing subunit with more than half of the maximal response magnitude among all residues are labeled. Residue numbering is consecutive across all subunits for each clamp protein.

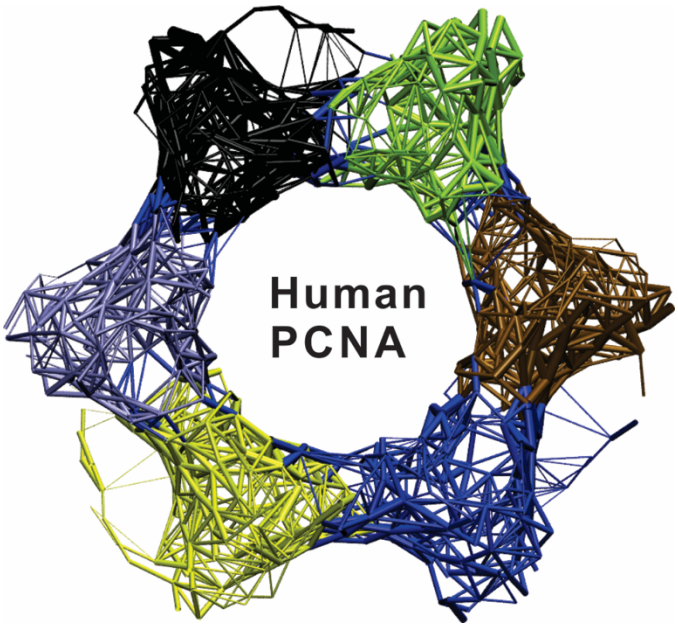

Figure S12. Dynamic network analysis identified communities in the human PCNA clamp.

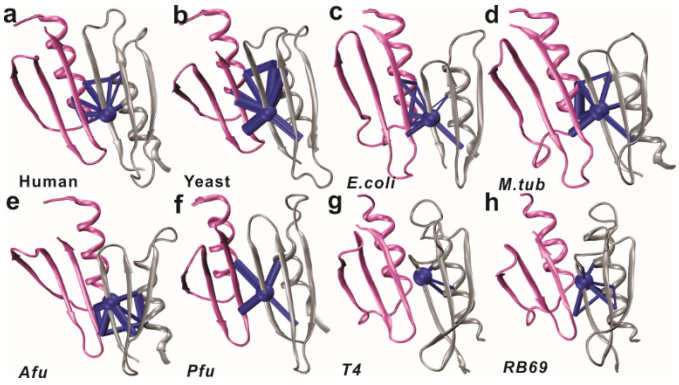

Figure S13. Dynamic communication at the clamp subunit interfaces identified from dynamic network analysis. a) Human PCNA; b) Yeast PCNA; c) *E. coli* β-clamp; d) *M. tub* clamp; e) *Afu* PCNA; f) *Pfu* PCNA; g) *T4* gp45; h) *RB69* gp45. The clamp protein subunits are shown in cartoon and colored accordingly. The Cα of the Tyr or Phe anchor residue is shown in ball representation. The number of edges going across the subunit interface indicates the extent of dynamic communication involving the hydrophobic anchor residue. The width of the edges indicates betweenness.